

# MEMS ABSOLUTE PRESSURE SENSOR ON A FLEXIBLE SUBSTRATE

Moinuddin Ahmed<sup>1</sup>, Donald P. Butler<sup>1</sup> and Zeynep Celik-Butler<sup>1</sup>

<sup>1</sup>Department of Electrical Engineering and Nanotechnology Research and Teaching Facility,  
University of Texas, Arlington, Texas, USA.

## ABSTRACT

This paper describes the fabrication and characterization of micromachined, piezoresistive, absolute pressure sensors sandwiched between a flexible polyimide. The sensors are designed for structural health monitoring in aerospace applications. A suspended aluminum oxide diaphragm is utilized where nichrome (Ni-80%/Cr-20%) piezoresistive sensors are placed in a half Wheatstone bridge geometry to ensure a linear response and thermal stability. The sensitivity was found to be 1.51 nV/Pa with an average dynamic range of 8.31 MPa.

## INTRODUCTION

Pressure sensing has numerous applications in automotive, aerospace, industrial process control and telecommunication systems [1]. Moreover, micromachined pressure sensors embedded in a flexible polyimide substrate have potential applications in structural health monitoring and medicine which require the sensors to place in an intimate contact with the non-planar and curved surfaces.

There are several types of micromachined pressure sensors are available and are classified by their transduction method. Diaphragm-based optical pressure sensors have been reported which measure pressure induced deflections by Fabry-Perot interferometry [2, 3] and have high resolution and sensitivity but often suffer from temporal sensitivity problems [4]. Resonant beam pressure sensors operate by monitoring the resonance frequency of an embedded doubly clamped bridge [5] or comb drive [6] and exhibit good pressure sensitivity with low temperature sensitivity and good noise immunity. Capacitive pressure sensors based upon parallel plate capacitors have the advantage of increased pressure sensitivity and decreased temperature sensitivity but suffer excessive signal loss from parasitic capacitance [7]. Piezoresistive pressure sensors, mounted on or in a diaphragm, are the most widely used pressure sensing device [7]. Different metals and semiconductors have been utilized as piezoresistive materials in micromachined MEMS pressure sensors, including ruthenium dioxide [8], indium-tin-oxide (ITO) [9], nickel-silver (Ni<sub>x</sub>-Ag<sub>1-x</sub>) [10], palladium, gold and copper [11], tantalum nitride copper [12], germanium [13], amorphous carbon [14] and silicon [15]. Nichrome (Ni-Cr 80/20 wt%) is a good choice for pressure sensor applications because of its high resistivity, low temperature coefficient of resistance (TCR), commercial availability and low temperature dependence of gauge factor (GF). The TCR of nichrome films decreases with the increase of the film thickness and a constant GF value of 2.50 for film thickness 15 nm or above has been shown [16].

In the current work, we have fabricated micromachined nichrome piezoresistive absolute pressure sensors embedded in a flexible substrate. The piezoresistive pressure sensors are mounted in an aluminum oxide membrane which serves as a diaphragm. To protect oxidation of nichrome during micromachining, aluminum oxide was deposited on the piezoresistor. A thick layer of aluminum oxide was deposited to vacuum-seal the cavity under the membrane which supplies a reference pressure. In this paper, we describe the fabrication process of the micromachined absolute pressure sensors embedded in a flexible substrate and the pressure sensitivity.

## FABRICATION

All depositions in the fabrication process were performed by rf magnetron sputtering in an Ar gas environment at room temperature. All the sputtered layers were patterned using photolithography and liftoff. A silicon carrier wafer was used in the fabrication of the pressure sensors in the flexible substrate so that conventional semiconductor processing equipment could be employed. The step by step fabrication of the relative pressure sensor is shown in Fig. 1. First, 200-nm of Si<sub>3</sub>N<sub>4</sub> was sputtered onto a 4-inch silicon wafer [Fig. 1(a)]. The Si<sub>3</sub>N<sub>4</sub> provided passivation of the Si carrier wafer and improved adhesion of the subsequent polyimide flexible substrate. This was followed by forming the flexible substrate through spin-coating of liquid polyimide onto the wafer for four times to achieve the desired thickness [Fig. 1(b)]. The polyimide was cured to yield a final thickness of 35 μm. The polyimide was then coated with another layer of 400-nm-thick Si<sub>3</sub>N<sub>4</sub> [Fig. 1(c)]. This layer serves as a passivation layer for the polyimide, promoting adhesion between the polyimide and the subsequent layers used to fabricate the pressure sensor. This Si<sub>3</sub>N<sub>4</sub> layer defines the device plane in the structure. After that, a thin sacrificial layer was deposited by spin-coating photo-definable liquid polyimide onto the Si<sub>3</sub>N<sub>4</sub> passivation layer and patterned by photolithography [Fig. 1(d)]. The polyimide was cured to yield 0.5-μm thickness. This sacrificial layer was used to build a passage for the next thick sacrificial layer's removal and decrease the requirement for a thick sealing layer. Next, a thick sacrificial layer was deposited by spin-coating photo-definable liquid polyimide and patterned by photolithography [Fig. 1(e)]. The polyimide was cured to yield 7-μm thickness. This sacrificial layer was used to build the absolute pressure sensor cavity. Next, 150 nm of Al<sub>2</sub>O<sub>3</sub> membrane layer was deposited [Fig. 1(f)]. This layer is an important part of the pressure sensor and undergoes deflection with the applied pressure. After that, the 38-nm-thick nichrome (Ni-80%/Cr-20%)

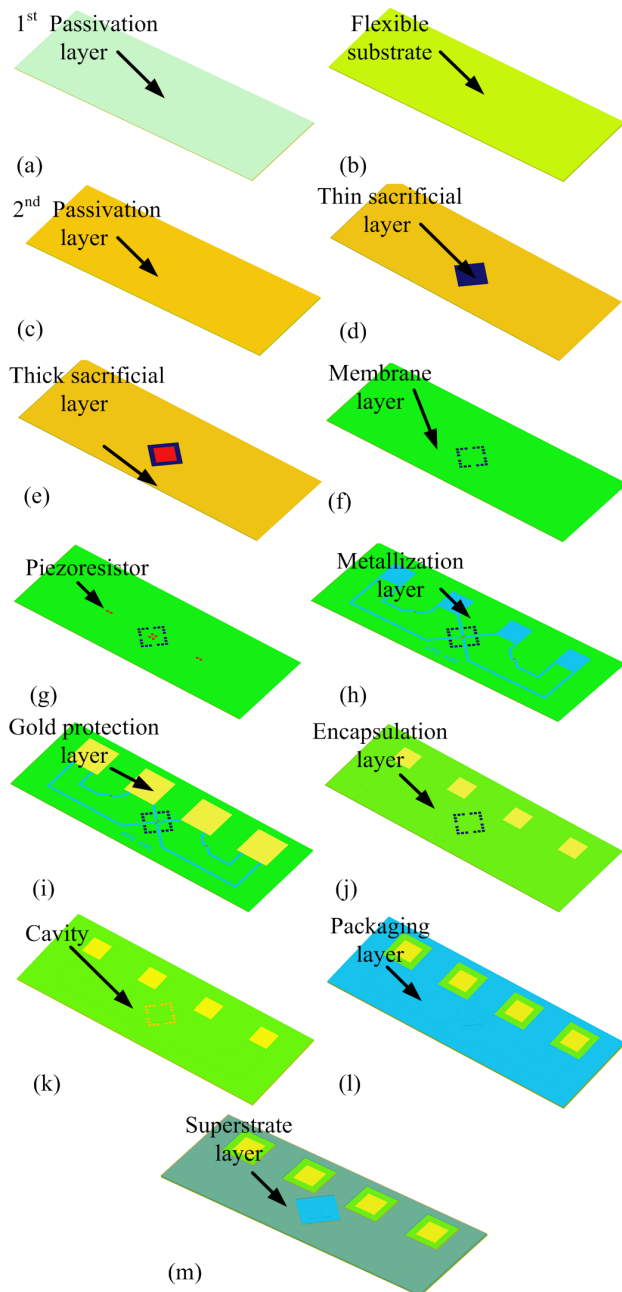


Fig. 1: Fabrication steps of absolute pressure sensor (a) 1<sup>st</sup>  $\text{Si}_3\text{N}_4$  passivation layer, (b) flexible substrate, (c) 2<sup>nd</sup>  $\text{Si}_3\text{N}_4$  passivation layer, (d) thin sacrificial layer, (e) thick sacrificial layer, (f)  $\text{Al}_2\text{O}_3$  membrane layer, (g) Ni/Cr piezoresistor, (h) Ti metallization layer, (i) Au contact pad, (j)  $\text{Al}_2\text{O}_3$  encapsulation layer, (k) Cavity created by micromachining, (l)  $\text{Al}_2\text{O}_3$  packaging layer, (m) superstrate layer.

piezoresistors were deposited [Fig. 1(g)]. Then, 2.15- $\mu\text{m}$  of Ti metallization layer was sputtered to connect the active and passive piezoresistors in a Wheatstone bridge geometry [Fig. 1(h)]. This was followed by depositing 200-nm of Au on top of the contact pads of the metallization layer [Fig. 1(i)]. The Au layer was used for wire bonding during the packaging of the absolute pressure sensors. Subsequently, 900-nm of  $\text{Al}_2\text{O}_3$  encapsulation layer was sputtered using rf-magnetron

sputtering [Fig. 1(j)]. This layer served to protect the piezoresistors and metallization from oxidation during the subsequent surface micromachining step. Afterwards, the sacrificial layers were removed by surface micromachining in an oxygen plasma with a Deiner Asher system to create a cavity under the membrane layer in the patterned region [Fig. 1(k)]. Next, the 3.5- $\mu\text{m}$ -thick  $\text{Al}_2\text{O}_3$  packaging layer was deposited using rf-magnetron sputtering. This layer sealed the cavity at 5 mTorr which serves as the reference pressure. Then, the packaging layer was etched using HF acid on a patterned area to open the contactpads for electrical connections [Fig. 1(l)]. Then, the superstrate layer was then deposited by spin-coating photo-definable liquid polyimide so that the sensor is at low stress plane [Fig. 1(m)]. The superstrate layer was patterned by photolithography to open vias for wire bonding and to expose the sensor region. The polyimide superstrate was cured to yield a 35- $\mu\text{m}$  thickness. The Coventor<sup>TM</sup> 3D model of the cross-section of the delta pressure sensor is shown in Fig. 2. The wafer was cut into small pieces and the pieces were packaged and wire bonded for characterization. The confocal microscope image of the completed devices is shown in Fig. 3. A 2x2  $\text{cm}^2$  piece of flexible substrate containing an array of 75 pressure sensors are shown in Fig. 4.

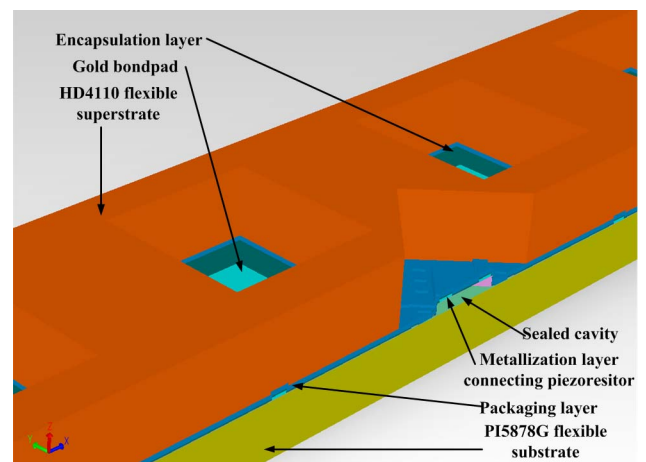


Fig. 2: The Coventor<sup>TM</sup> 3D model of the cross section of the absolute pressure sensor.

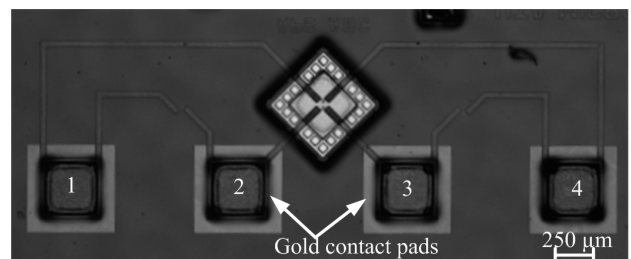


Fig. 3: Confocal microscope micrograph of the completed absolute pressure sensor.

## CHARACTERIZATION

The devices were wire bonded and characterized. A probe station equipped with a HP4155C semiconductor parameter analyzer was used to measure the current-



Fig. 4: A  $2 \times 2 \text{ cm}^2$  piece of flexible substrate containing an array of 75 pressure sensors.

voltage (I-V) characteristics. Resistors which were placed outside active region are called passive resistors and they are not substantially affected by the applied pressure. P1 and P2 are the passive piezoresistors whereas A1 and A2 are active piezoresistors placed on top of the membrane undergo strain in response to an applied pressure as shown in Fig. 3. Each individual resistance is in parallel with the three other resistances, hence the measurement of the I-V characteristic determines a pseudo resistance. Once the pseudo resistance values were measured using the slope of the I-V curve, the true values of the resistance were calculated using MATLAB.

The first characterization setup consisted of the XYZ manipulator stage on which the sample was placed. The stage could be moved along three axes and also be tilted. A tensile GS0-10 load-cell with varying loads of 0–10 g was utilized. The nanopositioner PI620-ZCD provided precise displacement of the probe tip, from 0–50  $\mu\text{m}$  in vertical direction, controlled by E-665 PZT Controller. A probe tip of radius of curvature  $r_p$  of 10  $\mu\text{m}$  was used for this characterization procedure. The sensor was electrically connected as described in the earlier section and input bias of 1 V was applied to the Wheatstone bridge. Again, the output offset voltage of the pressure sensor was measured with no applied pressure. The probe tip was then engaged onto the diaphragm surface by instructing the nanopositioner to move down in steps of 0.2  $\mu\text{m}$ . The load (in grams) and corresponding output voltage for each travel step was recorded. Then, the probe tip was moved up gradually and again the corresponding output voltages were measured [15]. The measurements were performed for two different configurations, again, which were obtained by switching input and output ports.

In a second characterization method, the pressure sensor was inserted into a vacuum chamber where a Welch duo-seal vacuum pump was used to create vacuum inside the chamber. The pressure inside the chamber was monitored using a Varian 715 vacuum pressure gauge. When pressure inside the chamber reached pressure of 100mTorr then the pump was turned off and the pressure inside the chamber increased slowly due to a leak in the system. The sensor was electrically connected as described in the earlier section and input bias of 1 V was applied to the Wheatstone bridge. As the pressure inside the chamber was increased, the corresponding output

voltage was measured using a Keithly 2182A Nanovoltmeter. The measurements were performed for two different configurations which were obtained by switching input and output ports and each measurements were taken two times.

## RESULTS AND DISCUSSION

The pseudo resistance values for each device measured during I-V characterizations are used to calculate individual resistance values. The resistances showed small variation with respect to each other due to lithographic abnormalities occurring during patterning and fabrication of the nichrome piezoresistor layer.

In the case of load-cell setup, the pressure sensor response characterized for the device named APID1-1A-ABCL is shown in Fig. 5. At higher pressures, it was observed that the change in output voltage saturates for a corresponding increase in pressure. This likely occurs as the membrane hits the bottom of the cavity. At this point, the diaphragm has maximum strain induced on the bridge arms. The sensor output was linear for small deflections corresponding to lower applied pressure. At higher pressure, small percentage of nonlinearity in sensor output was observed.

The device response in the vacuum chamber for the device termed as APID2-2A-ABC-R is shown in Fig. 6. The device showed quite linear response with the increase of pressure in the range of 100mTorr to 760 Torr and this response matched well with the design specification. The gauge factor for nichrome and Young's modulus was calculated as described by Ahmed *et. al.*[17]. The average value of the gauge factor for nichrome was found to be 1.95 and the Young's modulus of the rf sputtered  $\text{Al}_2\text{O}_3$  was calculated to be 406.67 MPa by Coventorware™ software.

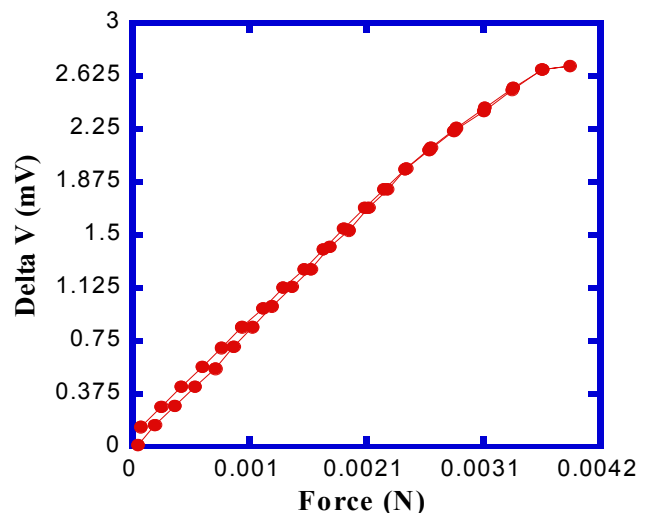


Fig. 5: Load-cell measurement for one of the absolute pressure sensors, showing output voltage change vs. applied pressure, depicting linear response until the membrane reaches the bottom of the cavity for a  $424 \mu\text{m} \times 424 \mu\text{m}$  device with 1V bias.

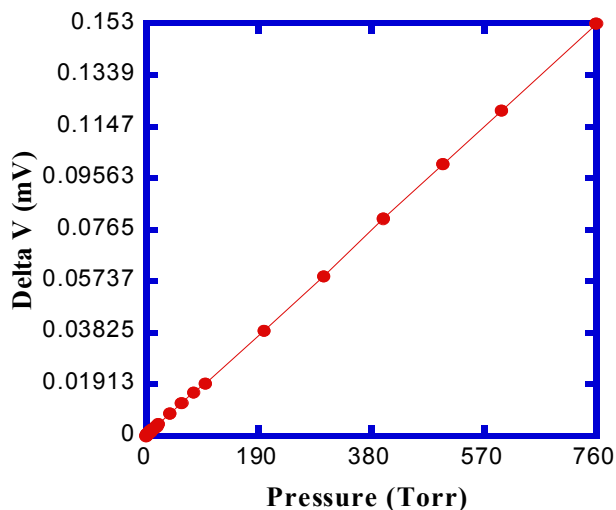


Fig. 6: Vacuum chamber measurement for one of the pressure sensors, showing output voltage change with respect to chamber pressure, depicting linear response for a  $424 \mu\text{m} \times 424 \mu\text{m}$  device with 1V bias.

## CONCLUSIONS

The fabrication and characterization of piezoresistive, absolute pressure sensor have been presented. Nichrome (Ni-80%/Cr-20%) was used as the sensing material and  $\text{Al}_2\text{O}_3$  was used as a membrane material. The average value of the gauge factor for nichrome was found to be 1.97 and the Young's modulus of the rf sputtered  $\text{Al}_2\text{O}_3$  was calculated to be 409.25 MPa. The average value of dynamic range was found to be 8.31 MPa and sensitivity was found to be 1.51 nV/Pa with 1V bias.

## ACKNOWLEDGEMENTS

The authors would like to thank Murali Chitteboyna for designing the masks used in this work. This material is based in part on work supported by L-3 Communications, Lockheed Martin Corporation, and the Air Force Office of Scientific Research (AFOSR) under Grant FA9550-06-1-0413.

## REFERENCES

- [1] N. K. S. Lee, R. S. Goonetille, Y. S. Cheung, G. M. Y. So, "A Flexible Encapsulated MEMS Pressure Sensor System for Biomechanical Applications," *Microsyst. Technol.*, vol. 7, pp. 55-62, 2001
- [2] G. C. Hill, R. Melamud, F. E. Declercq, A.A. Davenport, I. H. Chan, P.G. Hartwell, B. L. Pruitt, "SU-8 MEMS Fabry-Perot Pressure Sensor," *Sensor Actuat. A-Phys.*, vol. 138, pp. 52-62, 2007.
- [3] Y. Zhu, A. Wang, "Miniature Fiber-Optic pressure Sensor," *IEEE Photonic Tech. L.*, vol. 17, no. 2, pp. 447-449, 2005.
- [4] H. Bartelt, H. Unzeitig, "Design and Investigation of Micromechanical Bridge Structures for an Optical Pressure Sensor with Temperature Compensation," *Sensor Actuat. A-Phys.*, vol. 37-38, pp. 167-170, 1993.
- [5] K. Peterson, F. Pourahmadi, J. Brown, "Resonant Beam Pressure Sensor Fabricated with Silicon Fusion Bonding," in *Proc. 6th. Int. Conf Solid-State Sensor Actuat (Transducers '91)*, 1991, pp. 664-667.
- [6] C. J. Welham, J. W. Gardner, J. Greenwood, "A Laterally Driven Micromachined Resonant Pressure Sensor," *Sensor Actuat. A-Phys.*, vol. 52, pp. 86-91, 1996.
- [7] W. P. Eaton, J. H. Smith, "Micromachined Pressure Sensors: Review and Recent Developments," *Smart Mater. Struct.*, vol.6, pp. 530-539, 1997.
- [8] Tamborin, S. Piccinini, M. Prudenziati, B. Morten, "Piezoresistive Properties of  $\text{RuO}_2$ -Based Thick-Film Resistors: The Effect of  $\text{RuO}_2$  Grain Size," *Sensor Actuat. A-Phys.*, vol. 58, pp 159-164, 1997.
- [9] O. J. Gregory, T. You, "Atability and Piezoresistive Properties of Indium-Tin-Oxide Ceramic Strain Gages," in *Proc. 2nd Int. IEEE Sens.Conf.*, pp. 801-806, 2003.
- [10] H. Chiriac, M. Urse, F. Rusu, C. Hison, M. Neagu, "Ni-Ag Thin Films as Strain-Sensitive Materials for Piezoresistive Sensors," *Sensor Actuat. A-Phys.*, vol. 76, pp. 376-380, 1999.
- [11] S. U. Jen, C. C. Yu, C. H. Liu, G. Y. Lee, "Piezoresistance and Electrical Resistivity of Pd, Au, and Cu Films," *Thin Solid Films*, vol. 434, pp 316-322, 2003.
- [12] C. M. Wang, J. H. Hsieh, C. Li, "Electrical and Piezoresistive Properties of TaN-Cu Nanocomposite Thin Films," *Thin Solid Films* vol. 469-470, pp. 455-459.
- [13] W. D. Edwards, R. P. Beaulieu, "Germanium Piezoresistive Element on a Flexible Substrate," *J. Scientific Ins.* vol. 2, ser. 2, pp 613-615, 1969.
- [14] E. Piener, A. Tibrewala, R. Bandorf, S. Biehl, H. Luthje, L. Doering, "Micro Force Sensor with Piezoresistive Amorphous Carbon Strain Gauge," *Sensor Actuat. A-Phys.*, vol. 130-131, pp. 75-82, 2006.
- [15] S. K. Patil, Z. Celik-Butler, D. P. Butler, "Nanocrystalline Piezoresistive Polysilicon Film by Aluminum-Induced Crystallization for Pressure Sensing Applications," *IEEE Trans. Nanotech.*, vol. 9, no.5, pp. 640-646, 2010.
- [16] I. H. Kazi, P. M. Wild, T. N. Moore, M. Sayer, "Characterization of Sputtered Nichrome Films for Strain Gauge Applications," *Thin Solid films*, vol. 515, pp. 2602-2606, 2006.
- [17] M. Ahmed, D. P. Butler, Z. Celik-Butler, "MEMS Relative Pressure Sensor on Flexible Substrate," in *Proc. 10th Int. IEEE Sens.Conf.*, pp. 460-463, 2011.

## CONTACT

\*Donald P. Butler, tel:+1-817-272-1305, dbutler@uta.edu